Liquid Crystals, Vol. 33, No. 1, January 2006, 91–98

Taylor & Francis
Taylor & Francis Group

A method to estimate the Leslie coefficients of liquid crystals based on MBBA data

HAIYING WANG†, THOMAS X. WU†, SEBASTIAN GAUZA‡, JANET R. WU‡ and SHIN-TSON WU*‡

†Department of Electrical and Computer Engineering, University of Central Florida, Orlando, Florida 32816, USA
‡College of Optics and Photonics, University of Central Florida, Orlando, Florida 32816, USA

(*Received 15 July 2005; accepted 29 September 2005*)

A new effective approach for estimating the Leslie coefficients of liquid crystals based on MBBA data is presented. Literature values of the temperature-dependent Leslie viscosity coefficients of MBBA are used to fit with the analytical functions of Leslie coefficients based on the Imura and Okano theory, and a set of constants in these functions are determined. The same functions are then applied to two high birefringence liquid crystal mixtures, E7 and UCF-2, to extract their Leslie coefficients based on their order parameters. Using the extracted Leslie coefficients, the simulation results agree very well with the experimental data.

1. Introduction

Leslie viscosity coefficients [1] are critical in the investigation of the dynamic response of liquid crystal (LC) devices when backflow exists. It is noted that in some important applications the backflow is inevitable. For example, in laser beam steering at $\lambda=1.55\,\mu m$, the required 2π phase change leads to $d\Delta n\sim1.55$ for a transmissive optical phased array (OPA) [2], where d is the cell gap, and Δn is the birefringence. This $d\Delta n$ requirement is ~3X higher than that of a visible wavelength. Moreover, due to the birefringence dispersion effect [3] the LC birefringence drops ~20% in the near IR region as compared with that at $\lambda=550\,nm$. In the interest of achieving a fast response time, the use of a thin LC cell containing a high birefringence LC is a favourable approach. Due to the thin cell gap, a relatively high ($10\,V_{rms}$) voltage is needed in order completely to reorient the LC directors. Under such a driving condition, backflow is inevitable in the dynamic response [4, 5].

However, the available data on the viscous properties of various LC materials are almost always incomplete. So far, the only complete set of the six Leslie viscosity coefficients was published about two decades ago by Kneppe *et al.* in their complicated rotating magnetic field experiments [6]. The LC compound studied was 4-methoxybenzylidene-4′*n*-butylaniline (MBBA). But MBBA is not practical for OPA applications because of its poor material stability. Presently, many high birefringence LC mixtures are based on cyano-biphenyl and -terphenyl compounds. To study the dynamical response of OPA, it is necessary to find an effective method to estimate the Leslie coefficients for high birefringence LC mixtures.

In this paper, we propose an effective method for estimation of the Leslie coefficients based on the MBBA data. We used the published temperature-dependent MBBA data to fit the analytical functions of the Imura and Okana (IO) theory [7] and determined constants in these functions. To obtain better fitting for α_1 and α_2, we modify the function for α_1 in IO theory by adding a third order term and replace the function of α_2 by that proposed by Wu and Wu [8]. We assume that these constants are almost invariant for liquid crystal materials. The obtained set of constants is then used to calculate the Leslie coefficients of E7 (Merck) and UCF-2 [9, 10] using their order parameters.

The paper is organized as follows. In §2, we review the theory of the dynamic response of a nematic LC including backflow and present the method to estimate the Leslie coefficients. In §3, we briefly describe the experimental methods. In §4, the accuracy of the method is validated by comparing the experimental results with the finite element method (FEM) simulation results using the extracted Leslie coefficients. The agreement between theory and experiment is excellent.

2. Theory

2.1. *Erickson–Leslie equation*

In the dynamic Fréedericksz transition of a homogeneous nematic cell, the azimuthal angle ϕ is constant so

*Corresponding author. Email: swu@mail.ucf.edu

Liquid Crystals
ISSN 0267-8292 print/ISSN 1366-5855 online © 2006 Taylor & Francis
http://www.tandf.co.uk/journals
DOI: 10.1080/02678290500446111

that the LC director can be solely described by the tilt angle $\theta(z,t)$. The motion of the LC director is coupled with the flow v in the x-direction. The evolution of θ and v under an applied voltage is governed by the following Erickson–Leslie equation [1, 11], which takes into account the balance of elastic and electric field-induced torques:

$$\begin{aligned} I\frac{\partial^2\theta}{\partial t^2}+\gamma_1\frac{\partial\theta}{\partial t} &= \left(K_{11}\cos^2\theta+K_{33}\sin^2\theta\right)\frac{\partial^2\theta}{\partial z^2} \\ &\quad +(K_{33}-K_{11})\sin\theta\cos\theta\left(\frac{\partial\theta}{\partial z}\right)^2 \\ &\quad +\varepsilon_o\Delta\varepsilon E^2\sin\theta\cos\theta \\ &\quad +\left(\alpha_2\sin^2\theta-\alpha_3\cos^2\theta\right)\frac{\partial v}{\partial z} \end{aligned} \tag{1}$$

where α_i are the Leslie viscosity coefficients, I is the inertia of the LC, θ is the polar angle of the LC director (the angle between the LC director and the xy-plane, as depicted in figure 1), K_{ii} are the Frank elastic constants, $\Delta\varepsilon$ is the dielectric anisotropy, and v is the flow velocity. In general, the inertial effect is much smaller than the elastic and viscous torques and can be neglected. Neglecting the inertial term, the flow velocity is governed by:

$$\frac{\partial}{\partial z}\left\{\left(\alpha_3\cos^2\theta-\alpha_2\sin^2\theta\right)\frac{\partial\theta}{\partial t} +\frac{1}{2}\begin{bmatrix}2\alpha_1\sin^2\theta\cos^2\theta+(\alpha_5-\alpha_2)\sin^2\theta \\ +(\alpha_3+\alpha_6)\cos^2\theta+\alpha_4\end{bmatrix}\frac{\partial v}{\partial z}\right\}=0 \tag{2}$$

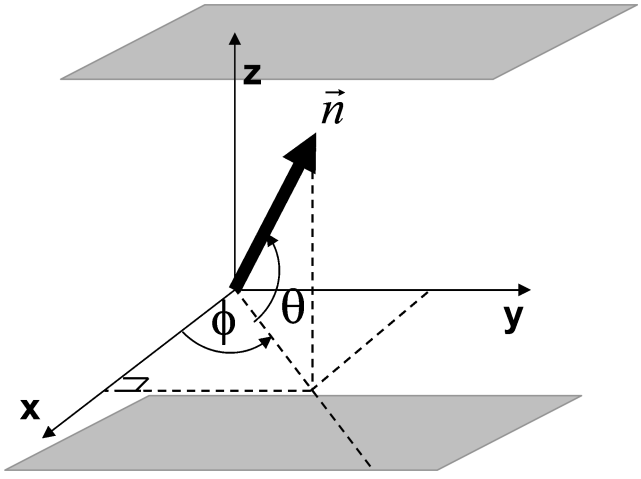

Figure 1. The coordinate system of the LC director, where θ is the tilt angle of the LC director, which is the angle between the LC director and the xy-plane, and ϕ is the angle between the projection of the LC director on the xy-plane and the x-axis.

Solving $\partial v/\partial z$ from equation (2), and substituting this into (1), we obtain the effective rotational viscosity γ_1^* as [12]:

$$\gamma_1^*=\gamma_1-\frac{\left(\alpha_2\sin^2\theta-\alpha_3\cos^2\theta\right)^2}{\frac{1}{2}\begin{bmatrix}2\alpha_1\sin^2\theta\cos^2\theta+(\alpha_5-\alpha_2)\sin^2\theta \\ +(\alpha_3+\alpha_6)\cos^2\theta+\alpha_4\end{bmatrix}} \tag{3}$$

where γ_1 is the rotational viscosity, and α_i are the Leslie coefficients. In the low voltage regime ($V<V_{th}$) of a homogeneous (splay mode) cell, γ_1^* can be approximated by γ_s^*, where [12]:

$$\begin{aligned}\gamma_s^*=\gamma_1^*(\theta=0)&=\gamma_1-\frac{2\alpha_3^2}{\alpha_3+\alpha_6+\alpha_4} \\ &=\gamma_1-\frac{2\alpha_3^2}{2\alpha_3+\alpha_2+\alpha_5+\alpha_4}.\end{aligned} \tag{4}$$

At a higher offset voltage ($V\gg V_{th}$), the LC directors are reoriented perpendicular to the substrates except for the boundary layers. Thus, the effective rotational viscosity (γ_B^*) for the bend mode ($\theta=90^\circ$) is [12]:

$$\gamma_B^*=\gamma_1^*(\theta=90)=\gamma_1-\frac{2\alpha_2^2}{-\alpha_2+\alpha_4+\alpha_5}. \tag{5}$$

It is evident from equations (4) and (5) that in a splay or bend mode operation, the LC director reorientation depends largely on α_2 and α_4+α_5; the α_3 values are one to two orders of magnitude smaller and are neglected. A similar effect is observed in the twisted nematic cell [13]. For laser beam steering, we need a pure phase modulator with phase change $\delta\geqslant 2\pi$. The pure phase modulation of a TN cell has been demonstrated in the low voltage regime, below the optical Fréederisckz transition threshold [14]. However, to achieve the required 2π phase change, the TN cell gap would be too large, so that the response time would be too slow. Both homogeneous and homeotropic cells can be used for pure phase modulation. However, from a molecular design standpoint it is easier to obtain LC compounds with a large and positive $\Delta\varepsilon$. Thus, in this paper we focus on the LC directors deformation of a homogeneous cell with strong anchoring at surface boundaries.

2.2. *Temperature effects*

Temperature has a great influence on the physical properties of a thermotropic LC. As temperature increases, the birefringence, dielectric anisotropy, viscosity, and elastic constant all decrease but at different rates. The temperature-dependent physical properties are mainly governed by the order parameter

S as [15]:

$$\Delta n = (\Delta n)_o S \tag{6a}$$

$$\Delta \varepsilon = A \frac{S}{T} \tag{6b}$$

$$K_{ii} = (K_{ii})_o S^2 \tag{6c}$$

$$\gamma_1 = bS \exp(E'/kT) \tag{6d}$$

where $(\Delta n)_o$ and $(K_{ii})_o$ are the birefringence and elastic constants, respectively, at $S=1$, i.e. $T=0$ K; A and b are proportionality constants, E' is the activation energy of molecular rotation, and k is the Boltzmann constant. If the temperature is not too close to the clearing point of the LC mixture T_C, the order parameter S can be approximated as [16]:

$$S = (1 - T/T_c)^{\beta} \tag{7}$$

equation (7) is Haller's approximation for the order parameter and β is a material constant. The ratio of $T_r = T/T_C$ is called the reduced temperature. This approximation holds quite well if the temperature is not too close to the clearing temperature ($T_C - T > 2^\circ$C). The exponent β is dependent on the molecular structure, but not on the wavelength. For most LC compounds studied, $\beta \approx 0.20$. For the E7 LC mixture we studied, $T_c \sim 58^\circ$C. From the measured temperature-dependent birefringence data, we obtain $(\Delta n)_o = 0.304$ and $\beta = 0.222$. These results are consistent with the published literature values [17].

2.3. *Temperature-dependent Leslie coefficients*

In the Imura and Okano theory, all six Leslie coefficients (α_1–α_6) are expressed in terms of the order parameter S as [7]:

$$\alpha_1 = A_1 S^2 \tag{8}$$

$$\alpha_2 = -(B_1 + C_1)S - (B_2 + C_2)S^2 \tag{9}$$

$$\alpha_3 = -(B_1 - C_1)S - (B_2 - C_2)S^2 \tag{10}$$

$$\alpha_4 = 2\eta_{is} - aS + A_3 S^2 \tag{11}$$

$$\alpha_5 = \left(\frac{3}{2}a + B_1\right)S + (A_2 + B_2)S^2 \tag{12}$$

$$\alpha_6 = \left(\frac{3}{2}a - B_1\right)S + (A_2 - B_2)S^2 \tag{13}$$

where the coefficients a, A_i, B_i and C_i ($i=1, 2$) are weakly dependent on the temperature. For different LC materials, for simplicity let us assume that these coefficients (a, A_i, B_i and C_i) remain unchanged but the order parameter would vary due to different β and T_C.

According to the definitions, $\gamma_1 = \alpha_3 - \alpha_2$ and $\gamma_2 = \alpha_6 - \alpha_5$. Based on the Parodi relationship [18], γ_2 can be rewritten as $\alpha_3 + \alpha_2$. In equation (11), η_{is} is the flow viscosity of the LC in the isotropic state

$$\eta_{is} = \eta_o \exp(E/k_B T) \tag{14}$$

where E is the activation energy of molecular diffusion, and η_o is a proportionality constant. Equation (14) is the well known Arrhenius law for isotropic liquids.

2.4. *Method for estimation of Leslie coefficients*

Based on the above discussion, we propose a method to estimate the Leslie coefficients. So far, the only complete set of Leslie coefficients was published for MBBA using the rotating magnetic field experiments [6]. Using the MBBA data to fit equations (8)–(14), we found $E = 0.414$ eV. During fittings, we have assumed that all the coefficients a, A_i, B_i and C_i ($i=1, 2$) are constants and used the recommended six Leslie coefficients of MBBA listed in table 1.

Using the MBBA data to fit the IO theory, we obtain a set of constants, listed in table 2. From these fittings, we find that the experimental data fit reasonably well with the IO theory for α_4, α_5 and α_6, but poorly for α_1, α_2

Table 1. Recommended Leslie coefficients for MBBA [9]. All α_i values are in units of Pa s. S is calculated from $S=(1-T/T_C)^{\beta}$ with $\beta=0.188$ and $T_c=46.2^\circ$C.

$T/^\circ$C	S	α_1	α_2	α_3	α_4	α_5	α_6
20	0.625	−0.0215	−0.1534	−.00077	0.1095	0.1071	−0.0471
25	0.600	−0.0181	−0.1104	−.00110	0.0826	0.0779	−0.0336
30	0.571	−0.0141	−0.0800	−.00151	0.0644	0.0572	−0.0244
35	0.533	−0.0095	−0.0573	−.00194	0.0515	0.0417	−0.0176
40	0.477	−0.0054	−0.0387	−.00223	0.0422	0.0285	−0.0124
42	0.443	−0.0036	−0.0310	−.00218	0.0394	0.0224	−0.0109
44	0.392	−0.0012	−0.0210	−.00179	0.0374	0.0136	−0.0092

Table 2. Parameters obtained from fitting MBBA data with the IO theory, equations (8)–(13). All the parameters are in units of Pa s.

A_1	B_1	C_1	B_2	C_2	η_o	a	A_2	A_3
−0.0417	−0.1442	−0.1568	0.4004	0.4179	4.33×10^{-9}	−0.0437	0.1729	−0.0829

and α_3. For α_1, a better fitting is found if we include a third order S term in equation (8):

$$\alpha_1=(A_4S+A_5)S^2 \tag{15}$$

where $A_4=-0.2072$ Pa s and $A_5=0.0748$ Pa s. The fitting result of α_1 using equation (15) is sketched in figure 2 (*a*), where the open circles and filled circles represent the measured and fitting results, respectively. The agreement is very good. Also included in figure 2 (*b*) for comparison are the fitting results using equation (8). Without the third order term, the fitting of equation (8) with experiment is quite unsatisfactory.

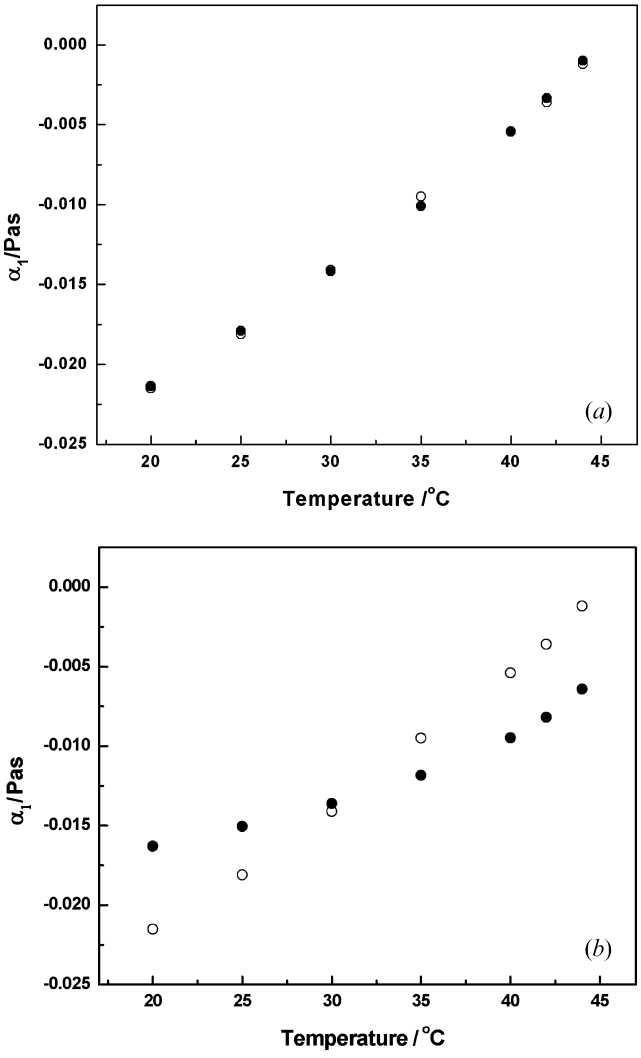

Figure 2. The fitting results of α_1 for MBBA (*a*) using equation (15) and (*b*) using equation (8). Open dots are measured data and filled dots are the fitting results.

The rotational viscosity is related to the Leslie coefficients (α_3 and α_2) as $\gamma_1=\alpha_3-\alpha_2$. From equations (9) and (10), we obtain the following expression for γ_1:

$$\gamma_1=2C_1S+2C_2S^2. \tag{16}$$

However, equation (16) does not fit the MBBA data well, as shown in figure 3. A better fitting is found using the following expression proposed by Wu and Wu [8]:

$$\gamma_1=bS\exp(E'/kT). \tag{17}$$

In equation (17), b is the proportionality constant, E' is the activation energy of molecular rotation, and k is the Boltzmann constant. From equation (17), the activation energy E', which is determined by the LC structures, has a dramatic effect on the rotational viscosity.

Figure 3 plots the MBBA data (dots) and fitting results using equations (16) (dashed lines) and (17) (solid line); it is clear that (17) has a much better fitting than (16). From table 1, the α_3 of MBBA is negative and much smaller than the other Leslie coefficients, which leads to:

$$\alpha_2\approx-\gamma_1=-bS\exp(E'/kT). \tag{18}$$

Thus, α_2 can be determined through the measurement of γ_1. Therefore, in our simulations we use the functional forms of equations (15) and (18) for α_1 and α_2, and equations (11)–(13) for α_4, α_5 and α_6, respectively. In the following, we will validate this method by comparing the experimental and simulation results using two LC mixtures, E7 and UCF-2. E7 was used in the first generation OPA; however, its figure of merit [19], defined as $FoM=K_{11}(\Delta n)^2/\gamma_1$, is only ~4 ms μm^{-2} at $T\sim48$°C. To enhance the FoM, we formulated a new mixture (UCF-2) consisting of isothiocyanato-tolane compounds. The FoM of UCF-2 reaches ~40 ms μm^{-2} at $T=70$°C. As a result, the OPA response time is improved by ~10X.

3. Experiment

In experiments, we measured the physical properties such as birefringence and visco-elastic coefficient of E7

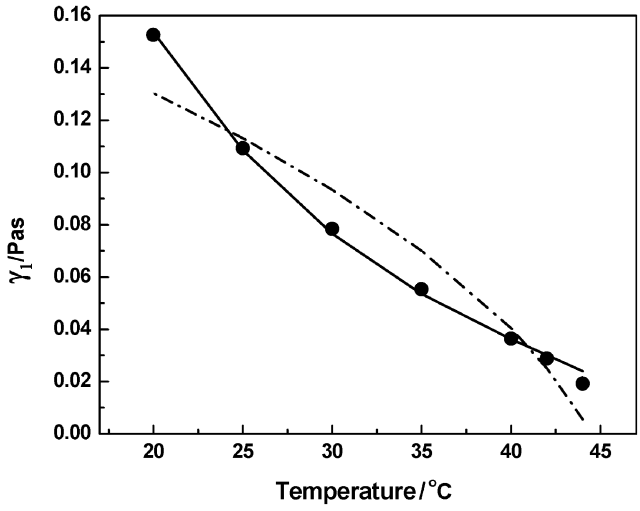

Figure 3. The temperature-dependent rotational viscosity of MBBA. Dots are the experimental data calculated from table 1, dashed lines are fitting results using equation (16), and solid line is fitting using equation (17).

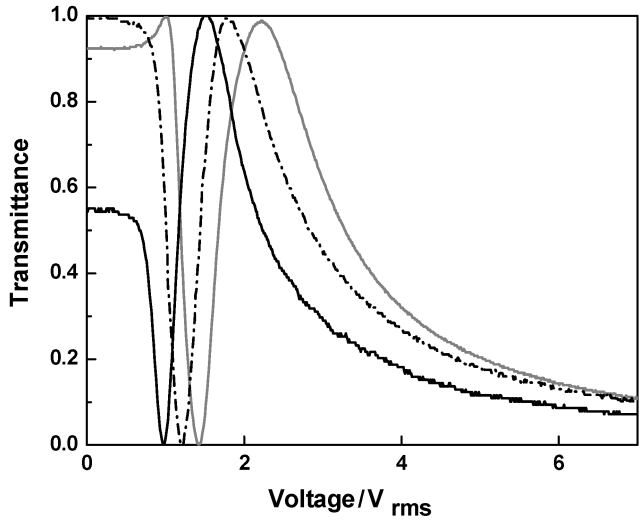

Figure 4. Voltage-dependent transmission of a 13.4 μm thick homogeneous E7 cell between crossed polarizers at three different temperatures: T=20.3°C (grey line), 33.3°C (dot-dashed line) and 46.9°C (solid line). λ=1.55 μm.

and UCF-2 using homogeneous cells. The inner sides of the indium tin oxide glass substrates were coated with a thin polyimide layer and then rubbed in anti-parallel directions. The buffing induced pretilt angle is ~3° and anchoring energy is $\sim 3 \times 10^{-4}\,\mathrm{J\,m^{-2}}$ [20]. The cell gap was determined from the transmitted interference fringes through a spectrophotometer and found to be d=13.4 μm for E7 and 7.81 μm for UCF-2. The elastic and dielectric constants of E7 and UCF-2 were measured using a computer-controlled APT III manufactured by Displaytech. The birefringence (Δn) was determined by measuring the voltage-dependent transmittance of the LC cell at λ=1.55 μm through a LabVIEW data acquisition system [21]. Table 3 lists the measured physical properties of E7 at T=20.3, 33.3, and 46.9°C, while table 4 is for UCF-2 at T=70°C.

For the temperature studies, the cell was held in an oven (INSTEC STC-200D) which has 0.2°C stability. To mimic the operating condition of an OPA, the LC cell was initially biased at V_i=10 V_{rms}. During the relaxation process, the voltage was removed at t=0 and the optical response monitored by a photodiode detector and displayed by a digital oscilloscope.

4. Results and discussion

To compare with the experimental results, we numerically solve equation (1) using the finite element method [22] and assume that the anchoring energy is infinite. The dynamic response of E7 and UCF-2 cells were studied.

4.1. *E7*

Figure 4 depicts the voltage-dependent transmittance curves at λ=1.55 μm and three different temperatures, T=20.3°C (gray line), 33.3°C (dot-dashed line) and

Table 3. Some measured and calculated LC parameters of E7 at various temperatures. λ=1.55 μm and T_c~58°C.

T/°C	K_{11}/pN	K_{33}/pN	$\varepsilon_{//}$	$\Delta\varepsilon$	Δn	α_1/mPa s	α_2/mPa s	α_3/mPa s	α_4 mPa s	α_5 mPa s	α_6/mPa s
20.3	11.7	19.5	19.6	14.5	.190	−21.2	−281.8	−1.0	224.7	92.1	−190.6
33.3	9.8	16.3	17	12	.175	−14.2	−123.5	−1.4	110.4	67.2	−57.7
46.9	7	10	15	10	.148	−6.2	−52	−1.9	70	34	−19.9

Table 4. Some measured and calculated LC parameters of UCF-02 at T=70°C and λ=1.55 μm.

T/°C	K_{11}/pN	K_{33}/pN	$\varepsilon_{//}$	$\Delta\varepsilon$	Δn	α_1/mPa s	α_2/mPa s	α_3/mPa s	α_4/mPa s	α_5/mPa s	α_6/mPa s
70	13.9	37.8	13.4	10.1	0.319	−25.9	−50.9	−0.7	72	107.9	56.3

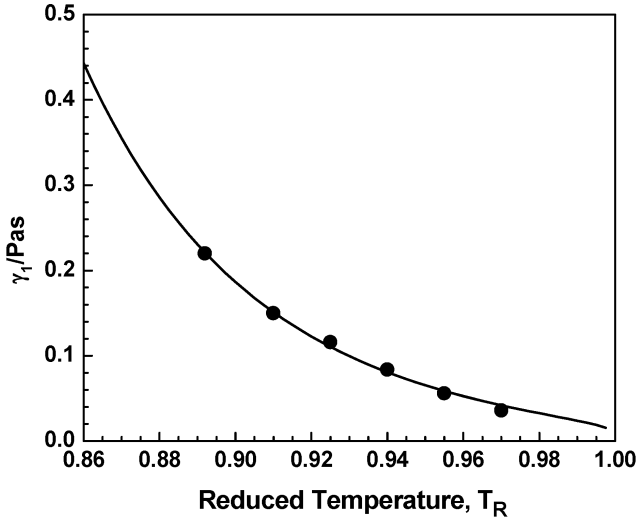

Figure 5. The temperature-dependent γ_1 of E7. Dots are measured data and solid line is the fitting curve using equation (17).

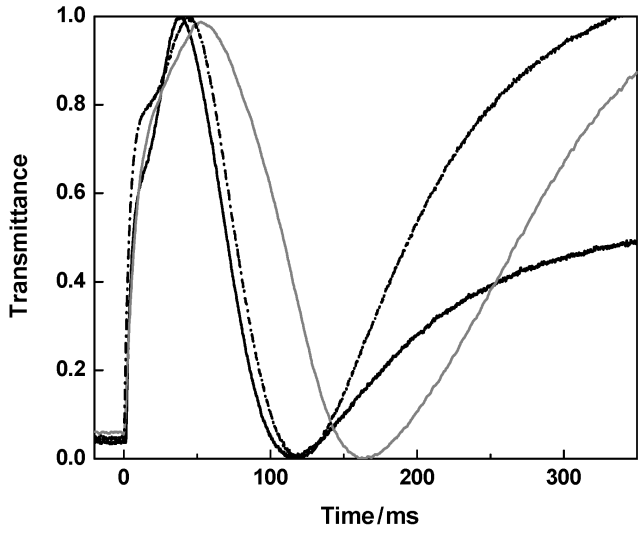

Figure 6. The experimental optical dynamic responses of a homogeneous E7 cell at three different temperatures: T=20.3°C (grey line), 33.3°C (dot-dashed line) and 46.9°C (solid line). d=13.4 μm and λ=1.55 μm.

46.9°C (solid line). From these curves, we find that the birefringence of E7 at λ=1.55 μm is Δn=0.190, 0.175, and 0.148 at T=20.3, 33.3, and 46.9°C, respectively.

The temperature-dependent rotational viscosity of E7 is shown in figure 5 where the dots are the measured data and the solid line is the fitting curve using equation (17). The measurement method for the rotational viscosity has been described in [17]. To fit the experimental data, we use the same β(=0.222) for the order parameter (S) and a, $\{A_i, B_i, C_i\}$ (i=1, 2), and A_3, A_4, and A_5 as MBBA and leave b and E' as adjustable parameters. From the fittings, we find $b=1.3\times10^{-8}$ Pa s and E'=0.439 eV for E7. The obtained activation energy agrees very well with that reported in [17] (E'=0.440 eV).

Figure 6 plots the measured optical dynamic response of the E7 LC cell at T=20.3°C (grey line), 33.3°C (dashed line) and 46.9°C (solid line), respectively. Before relaxation starts, the LC cell was biased at $V_b=10\,V_{rms}$. Under such conditions, the LC directors are reoriented almost perpendicular to the substrates throughout the bulk, except for the boundary layers. These boundary layers still retain a small residual phase retardation. Thus, under crossed polarizer conditions, a small transmittance at λ=633 nm is observed at t=0, as figure 6 shows. This residual transmittance is affected by the $d\Delta n$, threshold voltage, and surface anchoring energy of the LC cell. As the temperature increases, both birefringence and threshold voltage decrease. Thus, the initial transmittance becomes smaller. Moreover, the rotational viscosity decreases as the temperature increases. Thus, the time required to reach the first transmittance peak is reduced.

In figure 6, the backflow effect is clearly observed in the first few milliseconds. At the first stage of relaxation, the transmittance curve shows a steeper slope at each temperature due to the backflow effect. During the abrupt relaxation, the LC directors initially overshoot with time and attain a maximum value at a very short time before decaying monotonically to zero.

The transient optical dynamic response of the E7 cell at three different temperatures, T=20.3, 33.3 and 46.9°C, are shown in figure 7 (*a–c*), respectively. In these figures, the solid lines represent the experimental results and the dashed lines show the simulation results. The parameters used for the simulations are listed in table 3. The general agreement between the simulations and experimental results is quite good. As already discussed in theory, the director reorientation depends largely on α_2 and $\alpha_4+\alpha_5$ in the form of equation (4). In our simulations, we only adjusted the α_4 value to best fit the experimental results at each temperature. The values of α_4 in table 3 have already been updated for the best fittings. Here, we need to mention that the choice of α_4 is sensitive to the elastic constants, K_{11} and K_{33}. As the elastic constants increase, a larger α_4 is required to decrease the frictional torque, thus obtaining the new equilibrium between the elastic and viscous torques.

After having optimized the α_4 values at all three temperatures, we still use equation (11) for the fitting by only changing the activation energy of molecular diffusion. Figure 8 shows the fitting results. From the

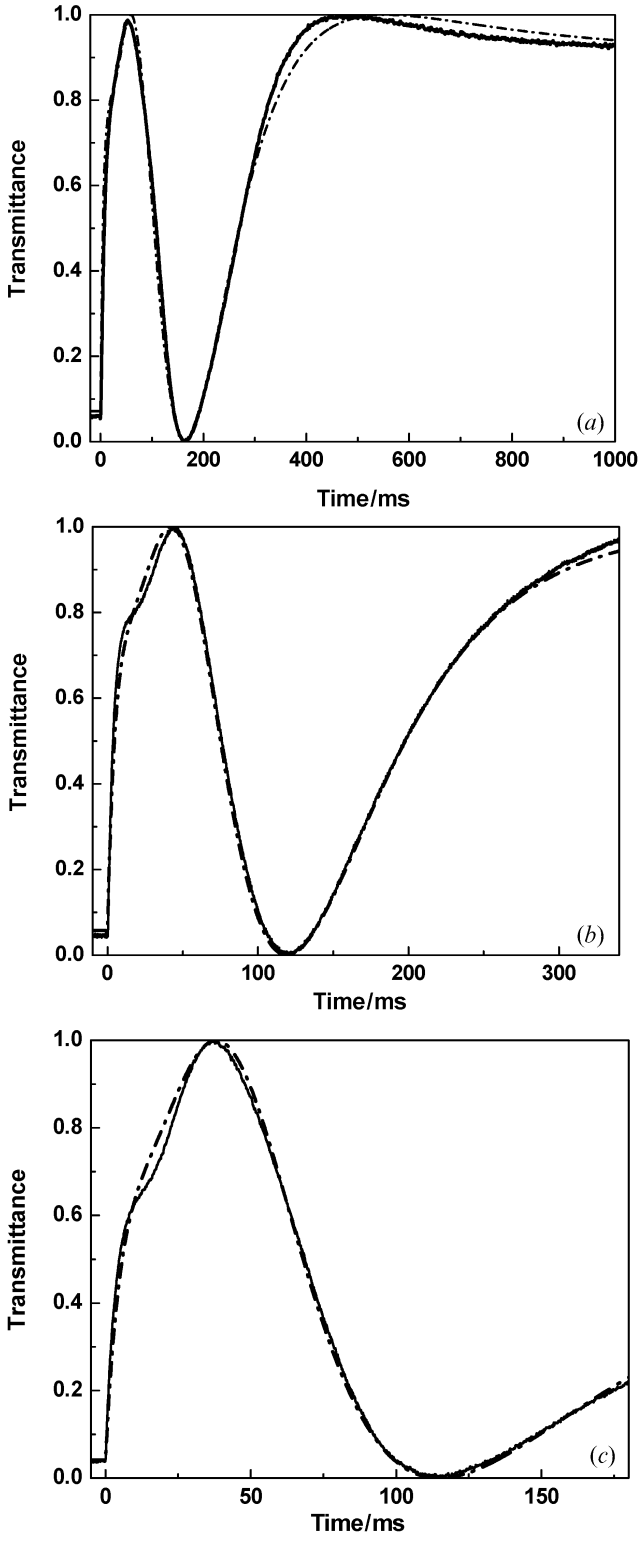

Figure 7. The transient optical dynamic responses of a homogeneous E7 LC cell at three different temperatures: (*a*) $T=20.3^{\circ}C$, (*b*) $T=33.3^{\circ}C$ and (*c*) $T=46.9^{\circ}C$. $d=13.4\,\mu m$ and $\lambda=1.55\,\mu m$. The solid lines represent the experimental results, while the dot-dashed lines are the simulation results. The parameters used for simulations are listed in table 3.

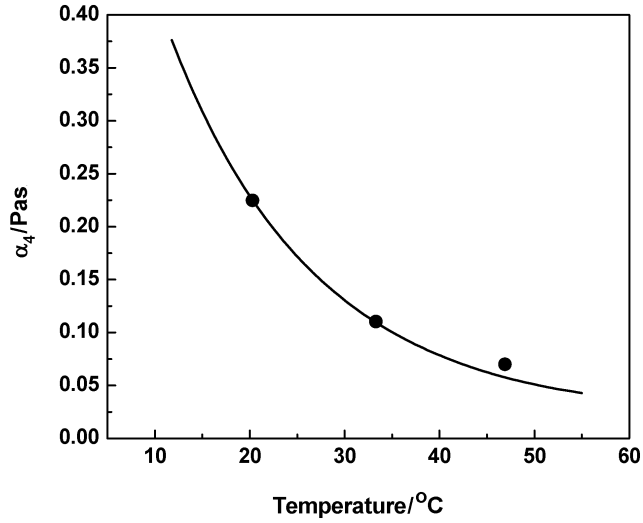

Figure 8. The temperature-dependent Leslie coefficient α_4 for E7. The solid line represents the fitting curve using equation (11) with $E=0.432\,eV$, while the dots represent the optimal values of α_4 at each temperature.

fittings, the activation energy (E) of the isotropic state can be extracted. For E7, we obtain $E=0.432\,eV$, which is comparable to that of MBBA ($E=0.414\,eV$) due to similar molecular conformations.

4.2. *UCF-2*

Further to verify the essential correctness of this approach we also tried the high birefringence LC mixture, designated as UCF-2, that we formulated. Its nematic range is 10.3–139.7°C. All the parameters used for simulations are listed in table 4. At $\lambda=1.55\,\mu m$ and $T=70^{\circ}C$, UCF-2 has $\Delta n\sim0.319$ which is about twice that of E7 at $T\sim47^{\circ}C$. Due to the higher birefringence, the required cell gap to achieve 2π phase change is reduced in proportion. By comparing table 4 with table 3, we find that the α_2 (or γ_1) of E7 at $T\sim47^{\circ}C$ is about the same as that of UCF-2 at $T=70^{\circ}C$. However, UCF-2 has a much higher clearing temperature than E7, which leads to a higher K_{11}. The visco-elastic coefficient (γ_1/K_{11}) of UCF-2 at $T=70^{\circ}C$ is one-third that of E7 at $T\sim47^{\circ}C$. As a result, UCF-2 has ~10 times higher FoM than E7.

Figure 9 plots the optical dynamic response of the UCF-02 LC cell ($d=7.81\,\mu m$) at $T=70^{\circ}C$. The simulation results (dashed line) fit very well with the experimental results (solid line). From the value of α_4, we find that $E=0.475\,eV$, which is ~10% higher than that of E7. Recall that E is the activation energy in the isotropic state. Although UCF-2 exhibits a lower viscosity than E7 in the nematic phase, its activation energy in the isotropic state is slightly higher than that

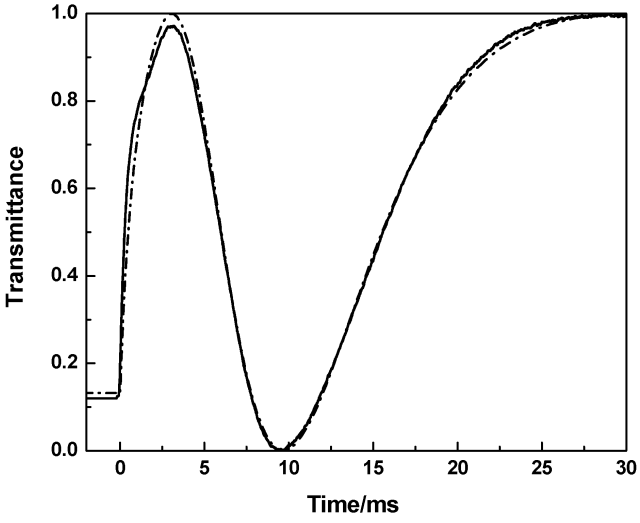

Figure 9. The transient optical dynamic responses of a homogeneous cell using UCF-02 LC mixture at $T=70^{\circ}C$. $d=7.81\,\mu m$ and $\lambda=1.55\,\mu m$. The solid line shows the experimental results and the dot-dashed lines are the simulation results. The parameters used for simulations are listed in table 4.

of E7. In the isotropic state, the inter-molecular association is much weaker and the cyanobiphenyl dimers are separated. The moment of inertia of cyanobiphenyl is smaller than that of isothiocyanatotolane, the major composition of UCF-2 [10]. As a result, E7 exhibits slightly smaller activation energy than UCF-2.

5. Conclusions

A new method for estimation of the Leslie coefficients of liquid crystals based on the MBBA data is presented. Fitting published temperature-dependent MBBA data into the analytical functions of the Imura and Okano theory on Leslie coefficients, a set of constants in these functions is obtained. Assuming these constants are invariant for different LC materials, the Leslie coefficients of other materials can be extracted based on their order parameters. The correctness of the approach is verified by excellent agreement between experimental results and simulation results using two kinds of high birefringence LC mixtures, E7 and UCF-2.

Acknowledgements

The authors are indebted to Yun-Hsing Fan, Yi-Hsin Lin, and H. Ren for the use of their experimental set-up and useful technical assistance. This work was supported by AFOSR under contract No. F49620-01-1-0377.

References

[1] F.M. Leslie. *Arch. ration. mechan. Anal.*, **28**, 265 (1968).
[2] P.F. McManamon, T.A. Dorschner, D.L. Corkum, L. Friedman, D.S. Hobbs, M. Holz, S. Liberman, H.Q. Nguyen, D.P. Resler, R.C. Sharp, E.A. Watson. *Proc. IEEE*, **84**, 268 (1996).
[3] S.T. Wu, U. Efron, L.D. Hess. *Appl. Phys. Lett.*, **44**, 1033 (1984).
[4] C.Z. van Doorn. *J. appl. Phys.*, **46**, 3738 (1975).
[5] D.W. Berreman. *J. appl. Phys.*, **46**, 3746 (1975).
[6] H. Kneppe, F. Schneider, N.K. Sharma. *J. chem. Phys.*, **77**, 3203 (1982).
[7] H. Imura, K. Okano. *Jpn. J. appl. Phys.*, **11**, 1440 (1972).
[8] S.T. Wu, C.S. Wu. *Liq. Cryst.*, **8**, 171 (1990).
[9] A. Spadło, R. Dąbrowski, M. Filipowicz, Z. Stolarz, J. Przedmojski, S. Gauza, Y.H. Fanand, S.T. Wu. *Liq. Cryst.*, **30**, 191 (2003).
[10] S. Gauza, H. Wang, C.H. Wen, S.T. Wu, A.J. Seed, R. Dąbrowski. *Jpn. J. appl. Phys., 1*, **42**, 3463 (2003).
[11] J.L. Erickson. *Trans. Soc. Rheol.*, **5**, 23 (1961).
[12] H. Schmiedel, R. Stannarius, M. Grigutsch. *J. appl. Phys.*, **74**, 6053 (1993).
[13] J. Kelly, S. Jamal, M. Cui. *J. appl. Phys.*, **86**, 4091 (1999).
[14] N. Konforti, E. Marom, S.T. Wu. *Opt. Lett.*, **13**, 251 (1988).
[15] W.H. de Jeu. *Physical Properties of Liquid Crystalline Materials*, Gorden and Breach, New York (1980).
[16] I. Haller. *Prog. solid state Chem.*, **10**, 103 (1975).
[17] S.T. Wu, C.S. Wu. *Phys. Rev. A*, **42**, 2219 (1990).
[18] O. Parodi. *J. Phys.*, **31**, 581 (1970).
[19] S.T. Wu, A.M. Lackner, U. Efron. *Appl. Opt.*, **26**, 3441 (1987).
[20] Y.H. Lin, H. Ren, Y.H. Wu, X. Liang, S.T. Wu. *Opt. Express*, **13**, 468 (2005).
[21] S.T. Wu, U. Efron, L.D. Hess. *Appl. Opt.*, **23**, 3911 (1984).
[22] J. Jing. *The Finite Element Method in Electromagnetics*, Wiley & Sons, New York (1993).